Nanotechnology Perceptions
ISSN 1660-6795
www.nano-ntp.com

Enhancing the Tribological Performance of SLM AlSi10Mg Through Parameter Optimization

Dr. P. Gandhi[1], Dr. G. Raja Kumar[2], Dharavath Saida[3], B. Venkanna[4], SK. Amer[5]

[1]Professor & Principal, Department of Mechanical Engineering, Kodad Institute of Technology and Science for Women, Suryapet Dt, Kodad– 508206, Telangana, India.
[2]Professor & Principal, Department of Mechanical Engineering, Swarna Bharati Institute of Science and Technology, Khammam, – 507002, Telangana, India.
[3]Lecturer in Mechanical Engineering, J.N.Govt Polytechnic, Ramanthapur,Medchal Malkajgiri, Hyderabad-500013, Telangana, India
[4]Assistant professor, Department of mechanical engineering, Sri Chaitanya Institute of Technology & Research, Ponnekal, Khammam-507170, Telangana, India
[5]Assistant professor, Department of mechanical engineering, Sri Chaitanya Institute of Technology & Research, Ponnekal, Khammam-507170, Telangana, India.
Email: gandhiperumallapalli@yahoo.co.in

In this Paper, the wear and mechanical properties of an AlSi10Mg alloy made by selective laser melting (SLM) were studied. The given process parameter influence of laser power energy densification behaviour and the effect of as build conditions on wear characterization were investigated. However, the wear and mechanical properties of the AlSi10Mg alloy showed better results than the Al6061-cast alloys. The SLM printed parts qualified for a structural geometric change from using the standard powder particle morphology (powder particle distribution range of 20 to 63 μm). The highest AlSi10Mg theoretical density of 2.67 g/cm3 and after SLM manufactured parts density was achieved by 99.6%. The laser energy density was calculated based on the given process parameter as 150 J/mm3.

The results obtained showed that the AlSi10Mg alloy had the lowest wear (both as built conditions) compared to the cast Al6061 material. Finally, at 200 rpm with a load of 60 N, the AlSi10Mg alloy produced the least wear rate of 1.39×10-8 mm2/N and a wear coefficient of 0.01mm2/N. The wear rate and wear coefficient increased as the slide speed increased. The hardness of the SLM-AlSi10Mg alloy Vickers was measured at 126±5 HV (as built).

Keywords: Laser Powder Bed Fusion (LPBF), Selective Laser Melting (SLM), AlSi10Mg alloy, Wear Characterization, Hardness, Microstructure.

1. Introduction

Additive Manufacturing (AM) techniques, such as Selective Laser Melting (SLM), have revolutionized the manufacturing industry by enabling the production of complex geometries and high-performance components. Among various materials, aluminum alloys, particularly AlSi10Mg, have emerged as promising candidates for AM due to their excellent mechanical properties, lightweight nature, and good corrosion resistance.

However, the successful implementation of SLM for AlSi10Mg requires a deep understanding of the influence of process parameters on the final product's quality and performance. Key process parameters, including laser power, scan speed, and layer thickness, significantly impact the microstructure, porosity, and mechanical properties of the fabricated components. These factors, in turn, directly affect the tribological behavior, such as wear resistance and friction coefficient, of the SLM-produced parts.

This research aims to systematically investigate the effect of process parameters on the tribological performance of AlSi10Mg alloy fabricated by SLM. By optimizing these parameters, it is possible to achieve superior wear resistance and mechanical properties, making SLM-produced AlSi10Mg components suitable for demanding applications in various industries, including automotive, aerospace, and biomedical.

The specific objectives of this study are:

- Microstructural Characterization: To comprehensively characterize the microstructure of AlSi10Mg alloys fabricated under different process parameters, focusing on the formation of intermetallic phases, porosity, and grain size.
- Mechanical Property Evaluation: To assess the mechanical properties, including hardness, tensile strength, and yield strength, of the SLM-produced AlSi10Mg alloys, correlating these properties with the underlying microstructure.
- Tribological Performance Testing: To evaluate the wear behavior of SLM-produced AlSi10Mg alloys under various loading conditions, including dry sliding and lubricated conditions, using standard tribological testing techniques.
- Process Parameter Optimization: To identify the optimal process parameters that lead to the desired tribological performance, considering factors such as wear resistance, friction coefficient, and component durability. These objectives, this research will contribute to the advancement of SLM technology for the production of high-performance AlSi10Mg components, enabling their widespread adoption in various engineering applications.

2. Literature Review

Early research on the SLM of AlSi10Mg primarily focused on process optimization and microstructural characterization. Kempen et al. [1], [2], [3] conducted pioneering work in this area, investigating the influence of process parameters such as laser power, scanning speed, and hatch spacing on the resulting microstructure and mechanical properties. Their research identified optimal process windows for achieving desired microstructures, including cellular, dendritic, and equiaxed grains, as well as optimal mechanical properties, such as tensile

strength, yield strength, and elongation. Buchbinder et al. [4], [5] further explored the potential of high-power SLM for AlSi10Mg and investigated strategies to mitigate distortion during the manufacturing process, including preheating techniques and optimized process parameter settings.

Subsequent studies delved deeper into the intricate relationship between process parameters, microstructure, and mechanical properties of SLM-produced AlSi10Mg. Delgado et al. [6] examined the impact of process parameters on part quality and mechanical properties for various materials, including AlSi10Mg. Read et al.[7] optimized the SLM process for AlSi10Mg and investigated the effects of different process parameters on mechanical properties, such as tensile strength, yield strength, elongation, and hardness. Rosenthal et al. [8] and Lam et al. [9] characterized the microstructure and phase composition of SLM-produced AlSi10Mg, providing valuable insights into the underlying mechanisms governing the solidification behavior and phase transformations.

The potential to enhance the mechanical properties of SLM-produced AlSi10Mg through heat treatment has been a subject of considerable interest. Aboulkhair et al. [10], [11], [12] investigated the precipitation hardening behavior of SLM-produced AlSi10Mg and the effects of conventional T6-like heat treatments on the microstructure and mechanical properties. Li et al. [13] studied the microstructure evolution, mechanical properties, and fracture mechanisms of SLM-produced AlSi10Mg after various heat treatment conditions, including solution treatment and aging.

In addition to mechanical properties, the tribological behavior of SLM-produced AlSi10Mg has been investigated. Zou et al. [14] studied the cavitation erosion behavior of SLM-produced AlSi10Mg, assessing its resistance to erosion damage under cavitation conditions. Wang et al. [15] examined the densification behavior and surface roughness of SLM-produced AlSi10Mg powders, which are crucial factors influencing the final part quality. Chen et al. [16] investigated strategies to improve the processability of complex geometries, such as overhanging structures, in SLM, enabling the fabrication of intricate components with high accuracy and minimal defects.

It is equipped with a 200W fibre laser, has a laser beam diameter of about 150 μm, using a scan speed of 1400 mm/s and a spacing of 105 μm. The density can be further increased to 99.8% by re-melting every layer with the same parameters, but alternating directions over 90°. The SLM AlSi10Mg parts have mechanical properties is higher comparable to the casted AlSi10Mg material, because of the very fine microstructure and fine distribution of the Si phase. SLM samples show some anisotropy in elongation at break. This is because of the optimal density scanning strategy which causes Z-oriented tensile samples to form more borderline porosity. These pores make the Z-oriented tensile parts more sensitive to crack initiation, compared to XY oriented tensile samples.

Delgado J et al. the current study provides an integrated set of experimental data, addressing key issues in part quality and mechanical properties. The general influence of the process parameters, such as scan speed, layer thickness, and build direction, has been investigated based on the statistical significance approach (ANOVA). The DMLS process parameters are layer thickness (LT) 0.02, 0.04 mm, scan speed (SS) 300, 360 mm/s and build direction (BD) 0°,90°. The SLM process parameters are layer thickness (LT) 0.03, 0.06 mm, scan speed (SS)

400, 500 mm/s and build direction (BD) 0°, 90°. The quality of parts produced by DMLS technology: The top surfaces (X–Y plane parallel to building platform) tend to have smoother finish compared to the lateral surfaces (Y–Z plane normal to the building platform). In terms of mechanical properties, the layer thickness factor (LT). An increase in layer thickness tends to weaken the parts in terms of tensile strength and elongation, with no effect on bending strength. In addition, the build direction has a significant influence on the bending strength and elongation, with no effect on tensile strength. The quality of parts is mainly influenced by the build direction and layer thickness factors.

Buchbinder D et al. investigation on reducing distortion by preheating during manufacture of aluminum components using selective laser melting. Independent of the material thicknesses, distortions can be reduced by using preheating in SLM test geometries made out of AlSi10Mg. Due to the preheating, the distortions of the test geometry (twin cantilever with bar thickness of 0.5 mm) are reduced from 10.6 mm (without preheating) to nearly zero (60.2 mm) at Tv=2500C within the scope of the measurement accuracy.

3. Methodology

3.1 Powder Characterization of AlSi10Mg

AlSi10Mg powder showing composite on Table 2.1 is provided by SLM solution Ltd. The offered powder size range 20-63 μm from SLM solution Germany.

Table 3.1: Chemical composition of AlSi10Mg

Al	Si	Fe	Cu	Mn	Mg	Zn	Ti	Ni	Pb	Sn	Other total
Balance	0.09	0.55	0.05	0.45	0.20 – 0.45	0.10	0.15	0.05	0.05	0.05	0.15

3.2 ASTM Specimen design

The sample prepared for SLM printing for wear characterization test specimen dimensions was 50 × 8 mm as shown in Figure 3.1.

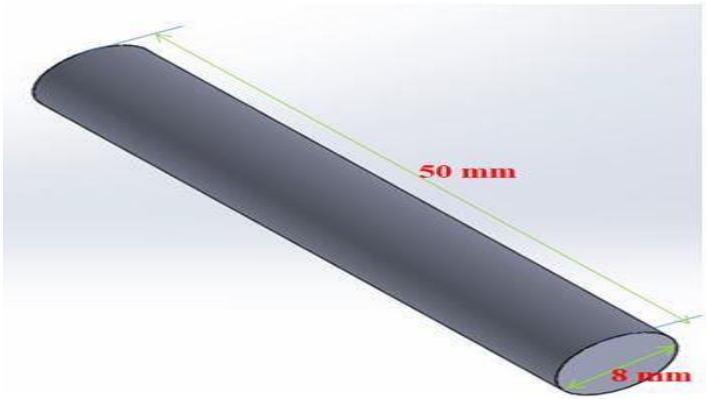

Figure 3.1: wear specimen

3.4 SLM PROCESS

The selective laser melting (SLM) uses a variety of alloys, allowing prototypes to be functional hardware made out of the same material as production components as shown in Figure 3.3 and specification of SLM as Table 3.1. Since the components are built layer by layer, it is possible to design organic geometries, internal features and challenging passages that could not be cast or otherwise machined. SLM produces strong, durable metal parts that work well as both functional prototypes or end-use production parts. The process starts by slicing the 3D CAD file data into layers, usually from 20 to 100 micrometers thick, creating a 2D image of each layer; this file format is the industry standard. stl file use most layer-based 3D printing or stereo lithography technologies. This file is then loaded into a file preparation software package that assigns parameters, values and physical supports that allow the file to be interpreted and built by different types of additive manufacturing machines. The selective laser melting, thin layers of atomized fine metal powder are evenly distributed using a coating mechanism onto a substrate plate, usually metal, that is fastened to an indexing table that moves in the vertical (Z) axis. This takes place inside a chamber containing a tightly controlled atmosphere of inert gas, either argon or nitrogen at oxygen levels below 500 parts per million. Once each layer has been distributed, each 2D slice of the part geometry is fused by selectively melting the powder. This is accomplished with a high-power laser beam, usually an ytterbium Fiber laser with hundreds of watts. The laser beam is directed in the X and Y directions with two high frequency scanning mirrors. The laser energy is intense enough to permit full melting (welding) of the particles to form solid metal. The process is repeated layer after layer until the part is complete. The SLM machine uses a high-powered 400 watt Yb-Fiber optic laser. Inside the build chamber area, there is a material dispensing platform and a build platform along with a recoated blade used to move new powder over the build platform.

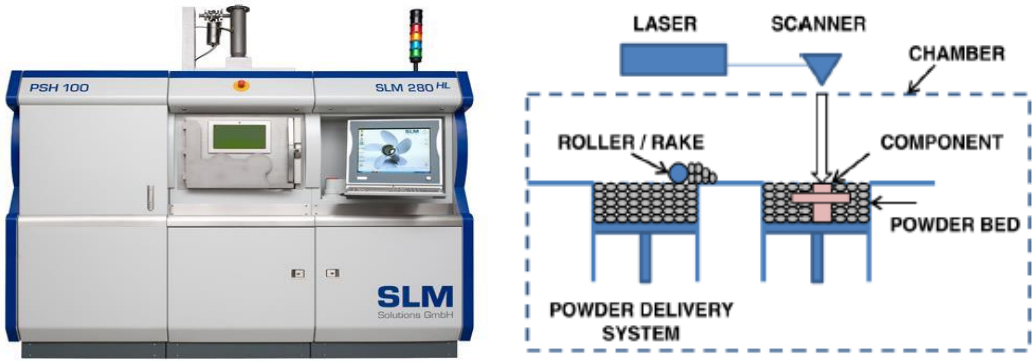

Fig 3.2: SLM process.

As per ISO/ASTM (52900-15) terminology SLM also referred to LPBF, is an AM technique developed to melt and fuse metallic powders via a high power-density laser. The principle of the SLM process starts with a building platform applied with very thin layers of metallic powders, which are completely melted later by the thermal energy induced by heat source with successfully binding. The cross-section area of the designed 3D part is built by selectively melting and re-solidifying metallic powders in each layer.

The building platform is then lowered by a small distance and a new layer of powders are

deposited and leveled by a re-coater as shown in Figure 3.4. The laser beam can be directed and focused through a computer-generated pattern by carefully designed scanner optics. Therefore, the powder particles can be selectively melted in the powder bed and form the shape of 3D objects according to the CAD (computer aided design). The SLM build platform dimensions have 280 × 280 × 365 mm and using a continuous IPG Fiber laser.

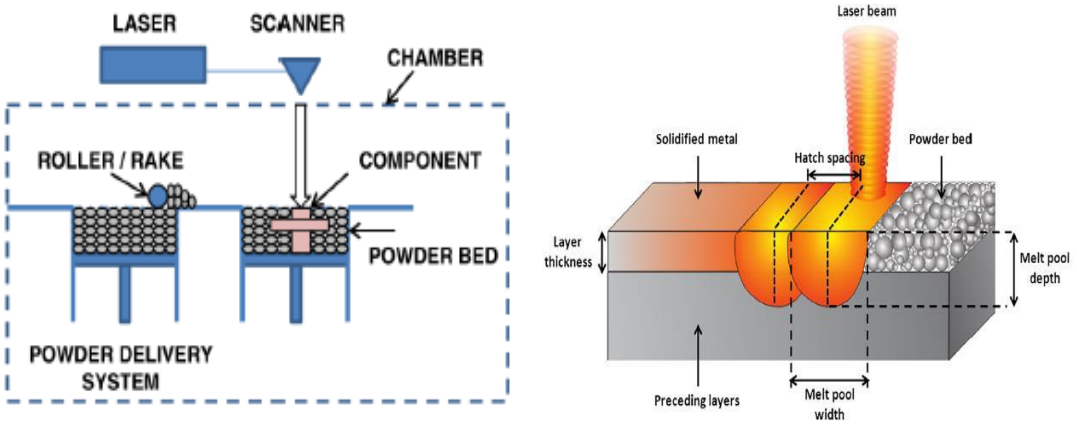

Figure 3.3: SLM schematic diagram and printing process.

3.5 Process Parameters:

3.5.1 Mesh Size and Build Material

- Build Mesh Size: This refers to the size of the elements used to discretize the 3D model of the part to be printed. A finer mesh size generally leads to more accurate simulations and better part quality, but it also increases computation time.
- Base Body Mesh Size: Similar to the build mesh size, but specifically for the base plate or build platform on which the part is printed.
- Build Material: The material used as the feedstock for the AM process. In the case of metal AM, this could be a metal powder like AlSi10Mg.

3.5.2 Directional Terms

- XY Direction: This refers to the horizontal plane of the build platform. In most AM processes, the laser or electron beam scans across this plane to melt and fuse the powder.
- Z Direction: This refers to the vertical direction, perpendicular to the build platform. It represents the layer-by-layer build-up of the part.

3.5.3 Temperature-Related Terms

- Preheat Temperature: The temperature to which the build platform is heated before the printing process begins. This can influence the thermal gradients during the build, affecting the final part quality.
- Deposition Thickness: The thickness of each layer of material deposited during the printing process.

- Gas Temperature: The temperature of the inert gas (e.g., argon) used to purge the build chamber and prevent oxidation.
- Powder Temperature: The temperature of the metal powder feedstock.
- Room Temperature: The ambient temperature of the environment surrounding the AM machine.

The design of experiment as per taguchi as shown in Table 3.2. The after manufactured specimens according to design of experiment as shown in Figure 3.4.

Parameters	Level 1
Laser power (LP) in Watts	300
Scan speed (SS) in mm/s	1000
Hatching distance (HD) in µm	150
Layer thickness	30 µm
Scanning direction	0º
Build orientation	0º
SLM chamber heat	150ºC

Table 3.2: Levels and their Factors for LPBF of AlSi10Mg alloy

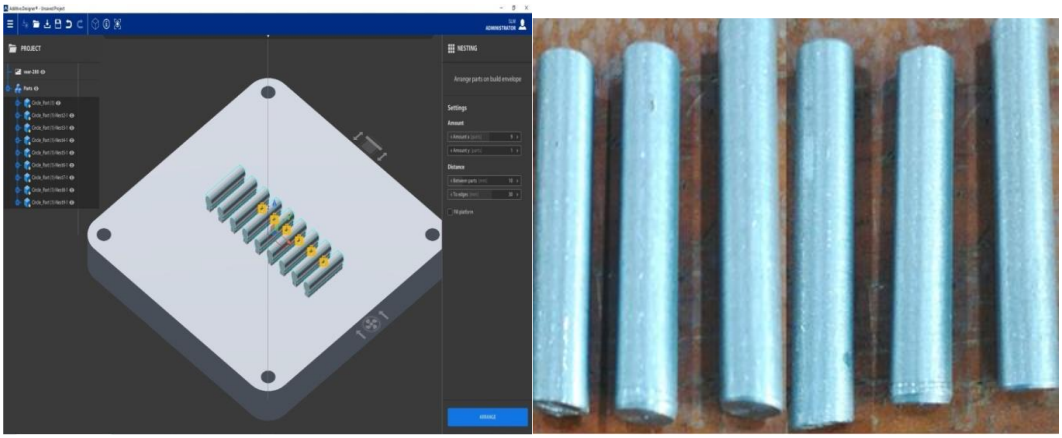

(a) (b)

Fig 3.4: a) Specimens on SLM build platform samples and b) After manufactured and casting specimens.

4. Result and Discussion

This work was studied as an optimization of process parameters with horizontal build orientation and conducted on a wear test of AlSi10Mg parts manufactured by SLM.

• Identified the suitable powder particle sizes for the SLM printing process.

• The key parameters of the SLM printing process were identified.

• Developed the simulation of the part before SLM printing.

• The output dynamic performance was conducted as a wear test.

• Find out the mechanical properties of hardness with microstructure characterization.

4.1 Wear characterization

The wear rate and wear coefficient of friction are frequently used to evaluate friction behavior. In this experiment, the disc was rotated from 200 to 600 rpm with a constant load of 60 N while keeping sliding track diameter constant at 80 mm and time 300 seconds. The testing was done at room temperature as shown in figure 4.1.

(a) (b)

Figure 4.1: (a&b) Wear testing schematic diagram

From the obtained wear and friction results, the speed, load, and time are used. Using these results, they calculated the percent (%) change of length, wear volume, wear velocity, wear rate, and wear coefficient as shown in the table 4.1.

Calculations:

➢ % change of length = Change in weight (wi – wf) / wi ×100 = % units

➢ Wear volume = Change in weight (wi – wf) / density of the material = mm3

➢ Wear velocity = 2πRN/60 (R= sliding distance 80 mm) = mm/s

➢ Wear rate = wear volume / wear velocity × load × time in sec. = mm2/N

➢ Wear coefficient = wear volume × hardness of material / R × load = mm2/N

Table 4.1: Wear calculation

results Wear Conditions	% change of length	Wear volume in mm^3	Wear velocity in mm/s	Wear rate in mm^2/N	Wear coefficient in mm^2/N
Case-I: 200 rpm					
As Casting Al6061	1.14	29.25	1647.67	9.86×10^{-7}	0.548
As 3D printed AlSi10Mg	0.10	1.35		4.47×10^{-8}	0.03

Case-II: 400 rpm					
As Casting Al6061	1.90	47.92	3349.33	1.11×10^{-7}	0.13
As 3D printed AlSi10Mg	0.17	1.85		3.06×10^{-8}	0.05
Case-III: 600 rpm					
As Casting Al6061	2.38	59.42	5024	6.75×10^{-7}	1.21
As 3D printed AlSi10Mg	0.18	2.14		2.36×10^{-8}	0.06

Wear rate ranges from 1.39 x 108 (minimum) to 9.86 x 10-7 mm^2/ N (maximum) and coefficient of friction ranges from 0.01 (minimum) to 1.21 mm^2/ N (maximum) for AlSi10Mg at different slide speeds. As the slide speed increases from 200 to 600 rpm, the maximum change in AlSi10Mg wear rate and co-efficient is shown in the figure 4.2.

(a)

(b)

(c)

Figure 4.2: (a) wear, (b) frictional force and (c) Coefficient friction

It shows that the coefficient of friction decreases as the sliding speed increases within the observation range as shown in figure 4.2. Increased surface roughness and large amounts of wear particles are believed to be responsible for the reduced friction associated with normal load increases.

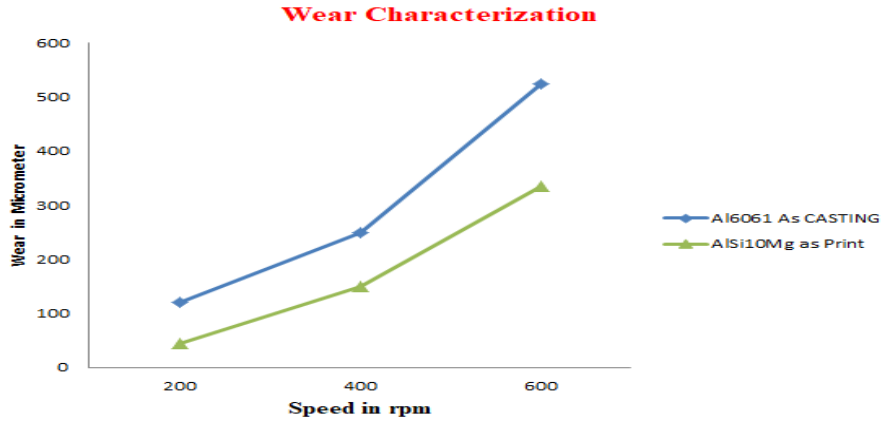

Graph 4.1: Wear characterization

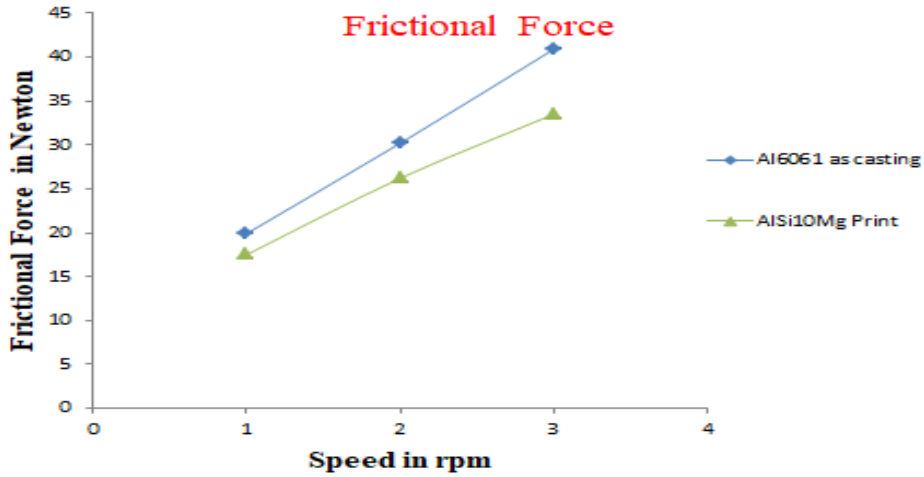

Graph 4.2: Frictional force results

4.2 Microstructure

The characterization of the microstructure evaluation was conducted by scanning electron microscope (SEM) at different magnifications and with high-resolution. The obtained microstructure used optimal process parameters and achieved a defect-free component with a high density of AM parts. The SEM was used for microstructure characterization at the different magnification levels as shown in figures 3.4 and Figure 3.5. In terms of strength and performance, the hatching distance was the most important factor. The pores can be divided into spherical pores and irregular pores, and cracks are observed along with the horizontal direction of the structure. Due to the poor wettability of oxides and metals, long cracks were formed and spread along the surface. Due to the low cooling rate, some of the AlSi10Mg

powder particles are formed as a result of oxidation during the SLM process.

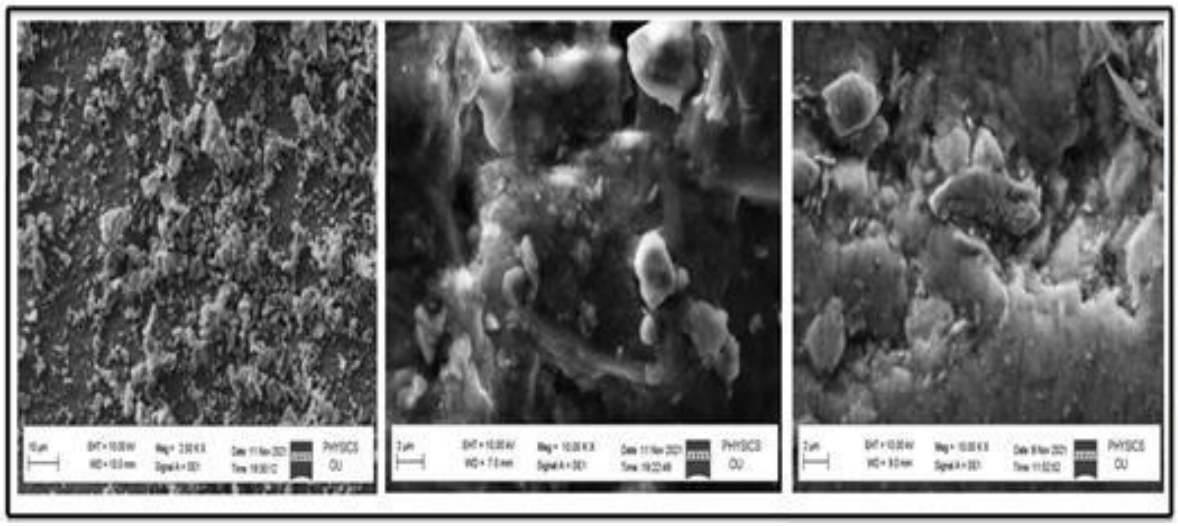

Figure 4.3: Microstructure of 300 watts/1000 mm/s with different magnifications.

4.3 Hardness

The Vickers hardness and density results are based on the optimized process parameters. The hardness and mechanical property values are mainly dependent on the microstructure of pores, cracks, and porosity with thermal deviation. The results of micro hardness tests under three different areas under an applied load of 1000 grams each held for 10 seconds are given in Figure 3.6 and table 3.6 and. The theoretical density of AlSi10Mg alloy powder (ρt) is 2.67 g/cm3 and, after SLM, manufactured parts have the highest density of 2.66 (99.6%) g/cm3.

Table4.3.1: Micro hardness results of AlSi10Mg and Al6061 alloy under the different conditions.

Different conditions	Micro hardness in HV
As-Built (SLM AlSi10Mg Printed sample)	126 ±5
As-Built (Casting Al6061 sample)	98±5

5. Conclusion

The AlSi10Mg alloy specimens were successfully manufactured by SLM-AM using optimized process parameters. The main results can be concluded as: The wear rate of the AlSi10Mg sample is about 33% lower than that of the cast Al6061 sample. The higher wear resistance of the AlSi10Mg sample with shallow and narrow wear grooves is due to the higher hardness induced by the unique binding of the microstructure with less pores and porosity defects.

• The obtained AlSi10Mg alloy wear test process parameters at As-build conditions were load

of 60 N, speed at 200 rpm, and time of 5 minutes, produced by low wear and friction compared to Al6061.

• The hardness of the AlSi10Mg alloy is better than that of Al6061, such as the As-build condition from 126 ±5 to 98±5 HV and

• The theoretical density of AlSi10Mg alloy powder by SLM solution (t) is 2.67 g/cm3.

References

1. Kempen K, Thijs L, Yasa E, Badrossamay M, Verheecke W, and Kruth JP, "Process Optimization and Microstructural Analysis for Selective Laser Melting of AlSi10Mg", In International Solid Freeform Fabrication Symposium, 2011.
2. Buchbinder D, Schleifenbaum H, Heidrich S, Meiners W, and Bültmann JJ, "High Power Selective Laser Melting (HP SLM) of Aluminum Parts", Physics Procedia, vol.12, pp.271-278, 2011.
3. Kempen K, Thijs L, Van Humbeeck J, and Kruth JP, "Mechanical Properties of AlSi10Mg Produced by Selective Laser Melting", Physics Procedia, vol.39, pp.439-446, 2012.
4. Delgado J, Ciurana J, and Rodríguez CA, "Influence of Process Parameters on Part Quality and Mechanical Properties for DMLS and SLM with Iron-Based Materials", International Journal of Advanced Manufacturing Technology, vol.60, no.5-8, pp.601-10, 2012.
5. Buchbinder D, Meiners W, Pirch N, Wissenbach K, and Schrage J, "Investigation on Reducing Distortion by Preheating During Manufacture of Aluminum Components Using Selective Laser Melting", Journal of laser applications, vol.26, no.1, pp.012004, 2014.
6. Kempen K, Thijs L, Van Humbeeck J, and Kruth JP, "Processing AlSi10Mg by Selective Laser Melting: Parameter Optimisation and Material Characterisation", Materials Science and Technology, vol.31, no.8, pp.917-923, 2015.
7. Read N, Wang W, Essa K, and Attallah MM, "Selective Laser Melting of AlSi10Mg Alloy: Process Optimisation and Mechanical Properties Development", Materials & Design, vol. 65, pp.417-424, 2015.
8. Rosenthal I, Nahmany M, Stern A, and Frage N, "Structure and Mechanical Properties of AlSi10Mg Fabricated by Selective Laser Melting Additive Manufacturing (SLM-AM)", In Advanced Materials Research Trans Tech Publications Ltd , vol. 1111, pp. 62-66, 2015.
9. Lam LP, Zhang DQ, Liu ZH, and Chua CK, "Phase Analysis and Microstructure Characterisation of AlSi10Mg Parts Produced by Selective Laser Melting", Virtual and Physical Prototyping, vol.10, no.4, pp.207-15, 2015.
10. Aboulkhair NT, Tuck C, Ashcroft I, Maskery I, and Everitt NM, "On the Precipitation Hardening of Selective Laser Melted AlSi10Mg", Metallurgical and Materials Transactions A,vol.46, no.8, pp.3337-41, 2015.
11. Li W, Li S, Liu J, Zhang A, Zhou Y, Wei Q, Yan C, and Shi Y, "Effect of Heat Treatment on AlSi10Mg Alloy Fabricated by Selective Laser Melting: Microstructure Evolution, Mechanical Properties and Fracture Mechanism", Materials Science and Engineering: A, vol.663, pp.116-125, 2016.
12. Liu YJ, Li SJ, Wang HL, Hou WT, Hao YL, Yang R, Sercombe TB, and Zhang LC, "Microstructure, Defects and Mechanical Behavior of Beta-Type Titanium Porous Structures Manufactured by Electron Beam Melting and Selective Laser Melting", Acta Materialia, vol.113, pp.56-67, 2016.
13. Aboulkhair NT, Maskery I, Tuck C, Ashcroft I, and Everitt NM, "On the Formation of AlSi10Mg Single Tracks and Layers in Selective Laser Melting: Microstructure and Nano-Mechanical

Properties", Journal of Materials Processing Technology, vol.230, pp.88-98, 2016.
14. Raus AA, Wahab MS, Shayfull Z, Kamarudin K, and Ibrahim M, "The Influence of Selective Laser Melting Parameters on Density and Mechanical Properties of AlSi10Mg", In MATEC Web of Conferences. vol. 78, pp. 01078, 2016.
15. Aboulkhair NT, Maskery I, Tuck C, Ashcroft I, and Everitt NM, "The Microstructure and Mechanical Properties of Selectively Laser Melted AlSi10Mg: The Effect of a Conventional T6-Like Heat Treatment", Materials Science and Engineering: A, vol.667, pp.139-146, 2016.
16. Chen T, Wang L, and Tan S, "Effects of Vacuum Annealing Treatment on Microstructures and Residual Stress of AlSi10Mg Parts Produced by Selective Laser Melting Process", Modern Physics Letters B, vol.30, no.19, pp.1650255, 2016.
17. Zou J, Zhu Y, Pan M, Xie T, Chen X, and Yang H, "A Study on Cavitation Erosion Behavior of AlSi10Mg Fabricated by Selective Laser Melting (SLM)", Wear, vol.376, pp.496-506, 2017.
18. Wang LZ, Wang S, and Wu JJ, "Experimental Investigation on Densification Behavior and Surface Roughness of AlSi10Mg Powders Produced by Selective Laser Melting", Optics & Laser Technology, vol.96, pp.88-96, 2017.